

Effects of Fan Installation on Ventilation in Indoor Sports Halls: A Numerical Simulation Study

Yanping Xiao^{1,2} and Xuanzhong Wu^{1,2,*}

¹ Fujian Key Laboratory of Intelligent Processing Technology and Equipment, School of Mechanical and Automotive Engineering, Fujian University of Technology, Fuzhou, 50100, China

² School of Mechanical & Automotive Engineering, Fujian University of Technology, Fuzhou, 350118, China

INFORMATION

Keywords:

Sports hall
natural ventilation
CFD simulation
fan regulation

DOI: 10.23967/j.rimni.2025.10.56233

Revista Internacional
Métodos numéricos
para cálculo y diseño en ingeniería

RIMNI



UNIVERSITAT POLITÈCNICA
DE CATALUNYA
BARCELONATECH

In cooperation with
CIMNE[®]

Effects of Fan Installation on Ventilation in Indoor Sports Halls: A Numerical Simulation Study

Yanping Xiao^{1,2} and Xuanzhong Wu^{1,2,*}

¹Fujian Key Laboratory of Intelligent Processing Technology and Equipment, School of Mechanical and Automotive Engineering, Fujian University of Technology, Fuzhou, 50100, China

²School of Mechanical & Automotive Engineering, Fujian University of Technology, Fuzhou, 350118, China

ABSTRACT

In this study, numerical simulations were conducted to investigate the changes in air circulation after the installation of fans in a large indoor sports hall. It was found that optimizing the arrangement of fans and the settings for doors and windows can significantly enhance air convection, improve the distribution of airflow, and increase the thermal comfort of athletes. The combination of natural ventilation systems with mechanical fans can further improve air quality and energy efficiency. These findings can provide practical recommendations for the design of sports halls, which are crucial for improving athletes' performance and comfort, as well as enhancing the experience of spectators and other users. The analysis results indicate that in Model 2, the average wind speed of Scheme 7 is 1.6% higher than that of Scheme 5, 11.5% higher than that of Scheme 6, and 34.3% higher than that of Scheme 8. Therefore, Schemes 7 and 5 are identified as the optimal solutions for Model 2. When comparing the optimal solutions of both models, it was found that the average wind speed of Scheme 7 is 1.6% higher than that of Scheme 5, and 12% higher than that of Scheme 1, making Scheme 7 the overall optimal solution.

OPEN ACCESS

Received: 17/07/2024

Accepted: 31/10/2024

Published: 07/04/2025

DOI

10.23967/j.rimni.2025.10.56233

Keywords:

Sports hall
natural ventilation
CFD simulation
fan regulation

1 Introduction

With the development of society and the economy, human activities have led to significant environmental damage, resulting in the frequent occurrence of extreme cold and hot weather conditions. In the current scenario of resource scarcity and energy constraints, coupled with the high energy consumption of air conditioning systems, fans become the optimal choice in impoverished regions that cannot afford air conditioning. Under hot environmental conditions [ambient air temperature (T_{ambient}) $> 30^{\circ}\text{C}$] and humid conditions [relative humidity (RH) $\pm 70\%$], the combination of environmental heat stress and heat produced by exercise can exceed the body's heat dissipation capacity, leading to an increase in core temperature which subsequently reduces athletic performance. Therefore, it is essential to enhance indoor air velocity in sports halls. Finite element analysis can be used in building design to significantly reduce experimental costs and time. It enables the selection of the optimal solution

*Correspondence: Xuanzhong Wu (wxz@fjut.edu.cn). This is an article distributed under the terms of the Creative Commons BY-NC-SA license

by evaluating different operating conditions [1]. Through simulation and numerical optimization, the provided data can be used to predict climate [2]. Can reduce the cost of experiments that do not need to be performed under special circumstances [3], helping to prevent adverse factors and improve the quality of human life.

Current research, both domestically and internationally, mainly focuses on the impact of ventilation window opening methods on the natural ventilation inflow in sports halls. Li [4], for instance, emphasized this aspect in her study. Li [5] utilized Computational Fluid Dynamics methods to assess the effect of asymmetry in sports hall morphology on the wind speed at sports venues. Zhao et al. [6] used CFD methods to investigate the impact of ventilation window positions on indoor thermal comfort and air age in sports halls. The primary focus is on the influence of the shape of ventilation openings and the building form of sports halls on indoor ventilation effectiveness.

While natural ventilation is frequently regarded as a more sustainable solution than mechanical ventilation, it has notable limitations in predictability, controllability, and heat recovery. Even though natural ventilation has many favorable characteristics, it cannot meet all ventilation needs, and mechanical exhaust ventilation is relatively simple and has low installation costs [7]. Consequently, integrating mechanical and natural ventilation can effectively improve indoor air circulation and reduce carbon dioxide levels. The study by Elhadary et al. [8] considered the combined effect of mechanical and natural ventilation, specifically examining the direction of airflow from wall exhaust fans and rooftop fans.

Natural ventilation has the potential to replace mechanical ventilation during the transition season, and a large number of studies have verified the energy savings of natural ventilation or hybrid ventilation combining natural and mechanical ventilation [9–11]. Depending on the local climate, the use of natural ventilation can save 20%~40% of energy consumption [12]. Theoretical analysis of natural ventilation phenomena is essential for designing an effective mixing system [13]. Mechanical ventilation methods are the most commonly used systems in factories and can also be applied in large stadiums [14], so a combination of natural and mechanical ventilation is necessary. And the effect of wall-to-window ratio on the interior should be taken into account, Li et al. [15] extracted 18 design parameters of gymnasium building for energy analysis and obtained that the high side window-to-window ratio has the highest sensitivity to energy consumption.

This paper builds on previous research and aims to investigate the impact on indoor air circulation by incorporating ceiling fans, designing different outgoing exhausts, and introducing a new windward angle. The objective is to calculate the optimal solution for improving the average indoor air velocity, thereby enhancing human athletic Effects of Fan Installation on Ventilation in Indoor Sports Halls: A Numerical Simulation Study.

2 Methodology

2.1 Model Establishment

To streamline the research, a model of a university sports hall was created. Various experimental control groups were established under identical boundary conditions. numerical simulation was utilized to simulate the wind environment, organizing the wind speeds at various inlets and outlets under natural ventilation and with the addition of fans. This process aimed to determine the optimal solution that maximizes the average indoor wind speed.

A model of a university sports hall was established with dimensions of 38.4 m in width, 77.9 m in length, and 13 m in height. As shown in Fig. 1, the numbering of doors and windows in the sports hall

is crucial for airflow analysis and optimization. The door openings (Nos. 22 and 23) are 2.7 m high and 2.6 m wide, while the door openings (Nos. 21 and 24) are 2 m high and 3.9 m wide. The windows on the left and right walls (Nos. 1, 2, 3, 4, 7, 8, 9, 10, 11, 12) are 1.75 m wide and 1.8 m high. The windows on the front and rear walls (Nos. 5, 6, 13, 14) are 1.55 m wide and 1.8 m high, with the lower edges of both sets of windows situated 4.8 m above the ground. The windows on the front and rear walls (Nos. 15, 16, 17, 18, 19, 20) are 3.9 m wide and 1 m high, with their lower edges 0.8 m above the ground.

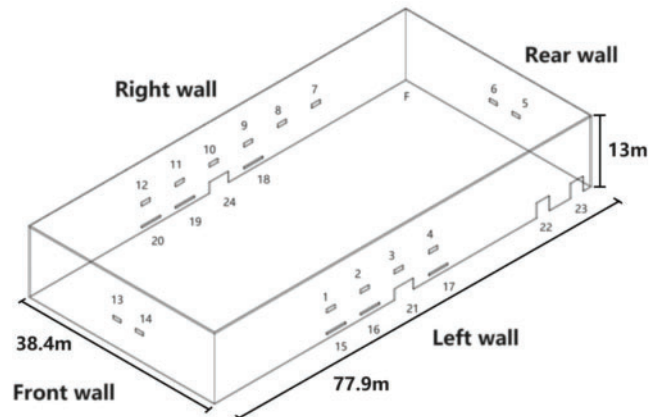


Figure 1: Numbering of doors and windows

Because the windows only open to 45 degrees, the window dimensions were scaled accordingly. The adjusted dimensions for the windows are as follows: for the left and right wall windows (Nos. 1, 2, 3, 4, 7, 8, 9, 10, 11, 12), the width remains the same, while the height is reduced to 680 mm; for the front and rear wall windows (Nos. 5, 6, 13, 14), the width remains unchanged, while the height is reduced to 600 mm; for the left and right wall windows (Nos. 15, 16, 17, 18, 19, 20), the width remains the same, while the height is reduced to 350 mm.

Four working conditions are selected to simulate the natural ventilation conditions under different door and window openings, and the optimal condition is selected for its optimization. The optimization scheme is optimized using fans, which are installed to further improve the effect of indoor ventilation to meet the requirements of comfort and health. Eight different optimization schemes are proposed, the installation of fans follows as much as possible uniform distribution on each wall, and the best ventilation scheme is found through different exhaust methods.

2.2 CFD Model and Parameter Setting

In this study, CFD numerical simulation method is used to simulate the ventilation characteristics of the indoor gymnasium, and the selected software is Fluent 2024 R1. Multi-faceted mesh is selected during meshing, and the mesh generating process encrypts the building part and the door and window part in order to improve the accuracy of the calculation of the internal and external fluids of the building, and the number of cells of the model of the final condition (a) was 1,790,839, and the number of nodes was 334,144, on the basis of the basic grid and set up two groups of control grid model, the number of cells in the rough group was 1,154,002, and the number of nodes was 216,686. The number of cells in the fine group was 2,790,484, and the number of nodes was 523,796. Comparing the average indoor wind speed of condition (a) under three grid sizes, the calculation shows that the maximum

error of the rough grid and the fine grid is 4.6%, which indicates that the number of base grids used in this paper meets the accuracy requirements.

The k-ε two-equation model is chosen, with the scheme set to Coupled and the flux type as Rhie-Chow: Distance Based. For spatial discretization, the gradient is set to Least Squares Cell Based, while pressure, momentum, turbulent kinetic energy, and turbulent dissipation rate are all set to Second Order Upwind. The model reaches a steady state after 3000 iterations, and all walls are non-slip wall surfaces.

2.3 Determination of Boundary Conditions

With the model dimensions set to length L, width W, and height H, the computational domain size is specified as $7L \times 5W \times 4H$ to ensure calculation accuracy. Thus, the model's fluid domain measures 545.3 m in length, 192 m in width, and 52.8 m in height. The distance between the model's inflow face and the inlet boundary is 150 m. The inflow boundary of the computational domain is defined as a velocity-inlet boundary, with reference to the Fuzhou city gradient wind coefficient. The gradient wind expression is given by $v = v_0 * (y/h_0)^n$, where h_0 and v_0 are the reference height and the wind speed at the reference height, respectively. Based on the meteorological averages for Fuzhou at 14:00 to 17:00 in July and August 2023, the wind direction is 25°, the air temperature is 30.3°C, and the air humidity is 75%. Values of 10 m and 2.23 m/s are selected as reference values [16]. y and v represent a certain height in the fluid domain and the corresponding average wind speed at that height, respectively. The wind speed profile is implemented using the User Defined Function (UDF) feature of Fluent through programming [17]. Considering that the outflow has nearly fully developed, a free outlet boundary is adopted at the outflow boundary. The detailed boundary conditions are shown in Table 1. The inlet and outlet positions of the wind are displayed in Fig. 2, which illustrates the airflow pathways critical for ventilation efficiency.

Table 1: CFD simulation boundary conditions

Boundary conditions	Place	Wall motion	Shear condition	Roughness model
Interface:	Wall, fan	Stationary wall	No slip	Standard
Wall:	Wall	Stationary wall	No slip	Standard
	Fan	Moving wall	No slip	Standard
Inlet:	Udf compiled gradient winds			
Outlet:	Outflow			

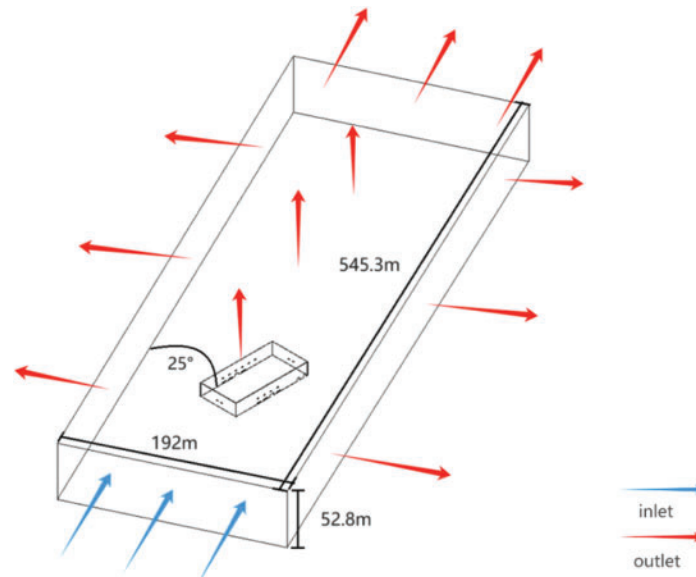


Figure 2: Inlet and outlet positions

3 Results

As summer progresses and temperatures rise, the temperature difference between the indoor and outdoor environments increases. Heat flows from outside through the windows into the interior, causing the indoor temperature to rise. However, as the indoor-outdoor temperature difference decreases, the effectiveness of convective airflow diminishes. Therefore, the ratio of wall windows affects indoor ventilation [18]. The manner in which doors and windows are opened in different directions influences wind pressure and wind direction, leading to changes in airflow paths and ventilation effectiveness. Selecting different opening methods for doors and windows in various directions can simulate the ventilation effects under different environmental conditions. Among these, cross-ventilation proves to be more effective than single-sided ventilation [19].

Four working conditions were designed based on an actual sports hall:

Condition (a): All doors and windows on the front, rear, left, and right walls are fully open.

Condition (b): The windows on the front and left walls are fully open, doors 22 and 23 are closed, and all doors and windows on the rear and right walls are fully open.

Condition (c): Doors 22 and 23 on the right side of the left wall are closed, all other doors and windows are fully open, the windows on the front wall are fully open, and windows 7 and 8 on the right wall are closed, making the ventilation area on the front and left walls consistent with that on the rear and right walls.

Condition (d): All doors and windows on the front, rear, and left walls are fully open, and windows 7, 9, and 11 on the right wall are closed.

3.1 Comparison of Wind Speeds at Windows

The model was simulated using Fluent. Wind pressure values were extracted at two heights, 1 and 5.1 m, at the midpoint of the windows. The wind pressure difference at these heights was calculated.

Four working conditions were set to select the optimal scheme, which was then further optimized by adding fans to enhance the ventilation effect. Detailed results are shown in [Tables 2](#) and [3](#).

Table 2: Average wind speed for each operating condition

Model	Inlet (m/s)	Outlet (m/s)		Inlet (m/s)	Outlet (m/s)	
Height	y = 1 m		Average wind speed (m/s)	y = 5.1 m		Average wind speed (m/s)
Condition (a)	1.486	0.467	0.977	1.566	0.475	1.021
Condition (b)	1.519	0.535	1.027	1.577	0.445	1.011
Condition (c)	1.600	0.439	1.019	1.571	0.499	1.035
Condition (d)	1.431	0.640	1.036	1.563	0.463	1.013

Table 3: Average differential wind pressure for each operating condition

Model	Inlet (pa)	Outlet (pa)		Inlet (pa)	Outlet (pa)	
Height	y = 1 m		Leeway (pa)	y = 5.1 m		Leeway (pa)
Condition (a)	0.190	−0.178	0.369	0.476	−0.143	0.619
Condition (b)	0.349	−0.215	0.564	0.573	−0.121	0.694
Condition (c)	0.289	−0.166	0.455	0.520	−0.162	0.682
Condition (d)	0.187	−0.313	0.500	0.471	−0.190	0.661

The analysis showed that at a height of 1 m, the average wind speed under Condition (d) is 6% higher than Condition (a), 0.8% higher than Condition (b), and 1.59% higher than Condition (c). At a height of 5.1 m, the average wind speed under Condition (a) is 0.7% higher than under Condition (d), Condition (c) is 2% higher than under Condition (d), and Condition (d) is 0.2% higher than under Condition (b).

3.2 Comparison of Wind Speeds at Sampling Points

The model was simulated using Fluent to obtain the wind speed results at the cross-sections of the front and rear windows of the model. As shown in the figure, Wind speed was sampled at intervals along the cross-section of the sports field, as illustrated in [Fig. 3](#), with a sampling height of 1.5 m to match the average chest height of standing individuals [20], as shown in [Fig. 3](#). The wind speed contour maps under different operating conditions, as shown in [Fig. 4](#), highlight the airflow patterns at varying heights.

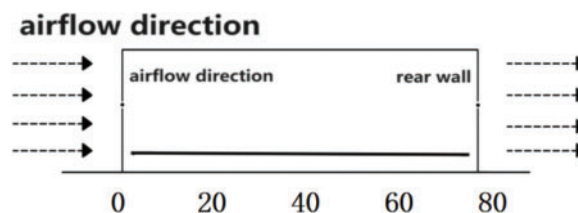


Figure 3: Wind speed sampling intervals

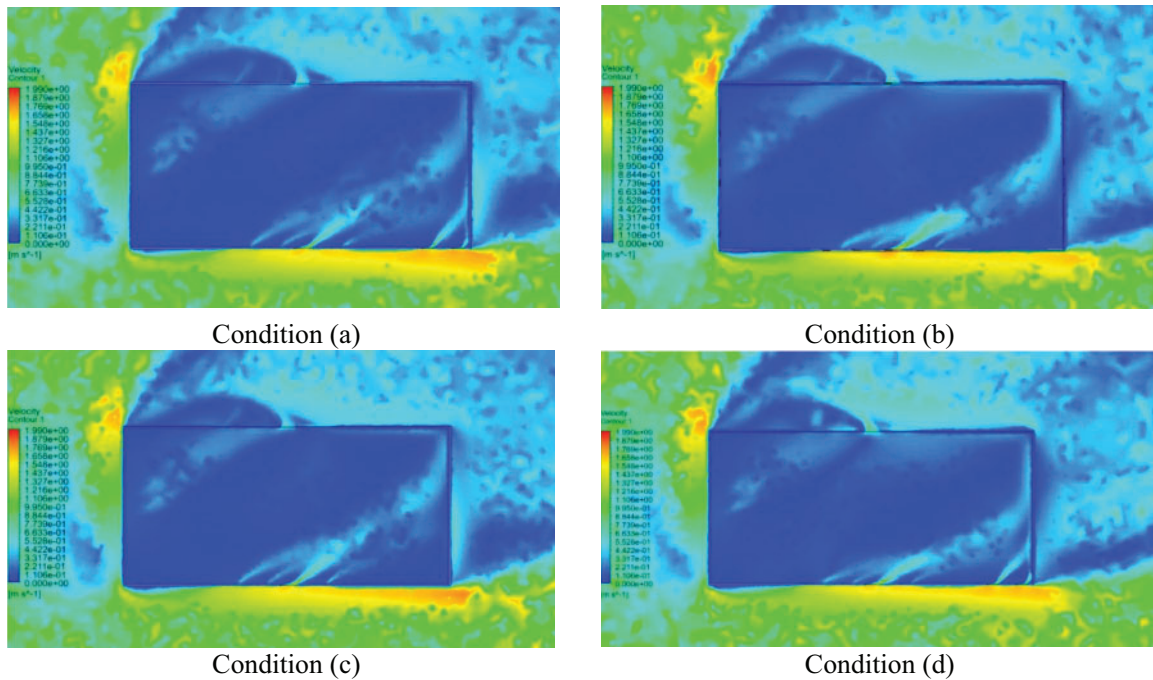


Figure 4: Wind speed contour maps

The wind speed analysis at a height of 1.5 m, presented in Fig. 5, provides detailed insights into airflow behavior under different ventilation scenarios. Observing the wind speed contour maps, it was found that the wind speed distribution in Condition (d) is more uniform and can cover the indoor area more comprehensively. The analysis showed that the average wind speed in Condition (d) is the highest, with Condition (c) being 18.7% lower, Condition (b) being 8.59% lower, and Condition (a) being 14.7% lower than Condition (d). According to Table 4, the national standard for wind speed in sports halls specifies that wind speeds less than or equal to 1.0 m/s fall within the range suitable for human activity areas [21].

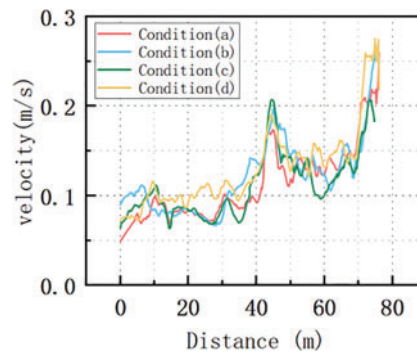


Figure 5: Wind speed analysis at 1.5 m

Table 4: Influence of wind speed on human motion

Wind speed (m/s)	Impact on humans and activities
0~<0.25	No sensation
0.25~<0.5	Comfortable
0.5~<1	Noticeable
1~<1.5	Noticeable ventilation
1.5~<7	Strong wind, affects activities

From the diagram, it can be observed that indoor wind speeds meet the requirement of ≤ 1.0 m/s, but where speeds are too low, they are less than 0.15 m/s, which is imperceptible to humans. Research indicates that in hot environments, athletes' performance is significantly affected, with a reduction in exercise duration by 16 ± 8 min and corresponding decreases in performance by $26 \pm 11\%$. Moreover, under conditions similar to Tokyo (which has a climate similar to Fuzhou), peak power output decreases by 0.5 ± 0.3 W/kg, corresponding to a reduction in performance by $16 \pm 7\%$ [22]. Given that university sports halls mainly cater to students, faculty, and the general public, there is no stringent requirement for facility conditions. However, in environments with low wind speeds, vigorous exercise can lead to respiratory discomfort and insufficient heat dissipation, increasing the risk of heat stroke. Analysis of the aforementioned conditions shows that condition (d) has the highest average wind speed, making it the optimal condition. Optimization of condition (d) is therefore recommended to enhance indoor airflow velocity.

3.3 Ventilation Optimization

To improve indoor ventilation rates and ensure a comfortable and healthy indoor environment, mechanical ventilation is desirable as it can accurately regulate indoor conditions in modern buildings. While natural ventilation is energy-efficient, it may not suffice to meet these requirements. The installation location and operating mode of fans significantly impact indoor airflow paths and speeds. By selecting different locations and operating modes, airflow can be optimized to enhance ventilation effectiveness [8]. Utilizing mechanical equipment is essential to optimize the sports hall. This study employed the installation of fans, considering both the expulsion of warmer air and the introduction of cooler air, resulting in a significant increase in indoor wind speed. Additionally, the method was designed to achieve the lowest energy consumption for fan operation. Based on a comparison of most fans and ceiling fans available on the market, the fan sizes chosen for this study are listed in Table 5. The fan model used for simulations is shown in Fig. 6, detailing the specifications and positioning of the fans.

Table 5: Specifications of the fan

Model	Diameter (mm)	Speed (rad/min)	Blades (pcs)
Fan (a)	760	1200	3
Fan (b)	6100	60	5

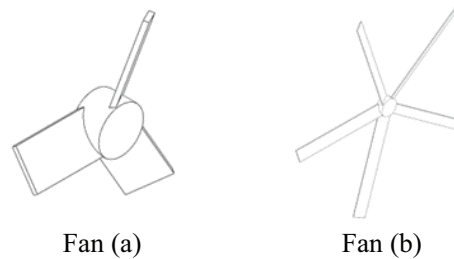


Figure 6: Fan model

Model 1:

For scenario (d), optimization is conducted with facade fan (a) installed at heights of 9.6 and 3.2 m. Fans are positioned on the left and right walls at intervals of 7.75 m, and on the front and rear walls at intervals of 6 m. Indoor fan (b) is installed at a height of 7 m. The indoor floor is divided into eight rectangles, with the center of fan (b) determined by the intersections of the diagonals of each rectangle.

Model 2:

For scenario (d), optimization is conducted with facade fan (a) installed at heights of 9.6 and 1 m. Fans are positioned on the left and right walls at intervals of 7.75 m, and on the front and rear walls at intervals of 6 m. Due to lower window positions preventing installation, six fans (a) are installed at a height of 2 m. Indoor fan (b) is installed at a height of 7 m. The indoor floor is divided into eight rectangles, with the fan (b) center determined by connecting the diagonals of each segment.

3.4 Grid Test

Optimization program selected software for Fluent 2024 R1. Grid division when the selection of multi-face mesh, grid generation process of the building part and the doors, windows and fans part of the encryption, in order to improve the accuracy of the calculation of the building inside and outside the fluid, the final number of cells of the model of the scheme 1 was 7,714,547, the number of nodes 1,366,463, in the basic grid on the basis of the set of two groups of control grid model, coarse the number of cells in the grid group was 5,574,909, and the number of nodes was 993,972. The number of cells in the fine grid group was 10,589,568, and the number of nodes was 1,929,660. Comparing the average indoor wind speed of Scheme 1 under the three kinds of grid sizes, the calculation shows that the maximum error between the coarse grid and the fine grid is 7.8%, which indicates that the number of basic grids used in this paper meets the accuracy requirements.

The k- ϵ two-equation model is chosen, and the couple algorithm is used, all of which are second-order equations, and the model reaches a steady state after 10,000 iterations, with non-slip walls for all walls and slip walls for the fans.

3.5 Optimization Schemes

Each fan is numbered, fans (a) are numbered 1–52. For simulation convenience, fan numbers skip over the left wall's number 16. Fans (b) are numbered 61–68.

Scheme 1: In Model 1, fans (a) numbered 1–8, 17–24, and 33–42 blow air indoors; fans numbered 9–15, 25–32, and 43–52 blow air outdoors. Fans (b) numbered 61–68 blow air towards the ground.

Scheme 2: In Model 1, fans (a) on the windward side blow air indoors (fans numbered 1–15, 33–42), fans on the leeward side blow air outdoors (fans numbered 17–32, 43–52). Fans (b) numbered 61–68 blow air towards the ground.

Scheme 3: In Model 1, fans (a) at a height of 9.6 m (odd-numbered fans on walls) blow air outdoors; fans at a height of 3.2 m (even-numbered fans on walls) blow air indoors. Fans (b) numbered 61–68 blow air towards the ground.

Scheme 4: In Model 1, fans (a) at a height of 9.6 m (odd-numbered fans on walls) blow air indoors; fans at a height of 3.2 m (even-numbered fans on walls) blow air outdoors. Fans (b) numbered 61–68 blow air towards the ground.

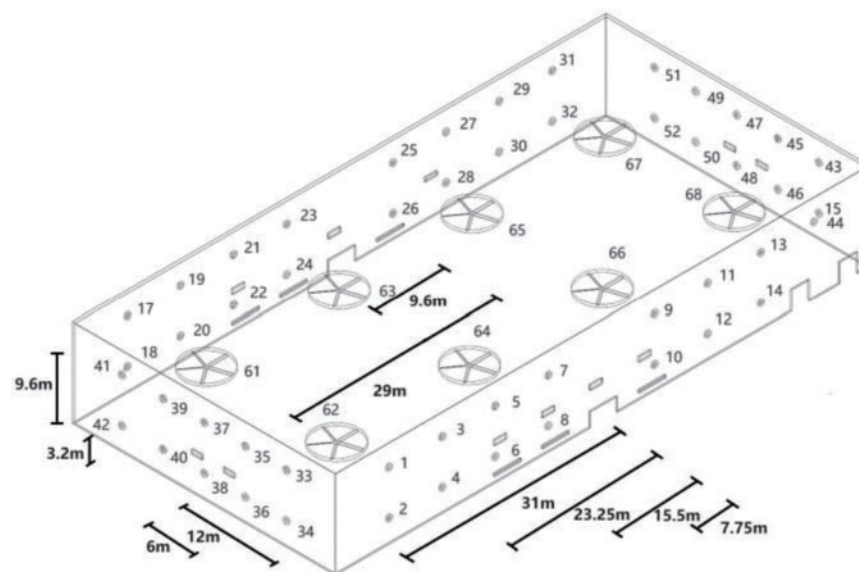
Scheme 5: In Model 2, fans (a) numbered 1–8, 17–24, and 33–42 blow air indoors; fans numbered 9–15, 25–32, and 43–52 blow air outdoors. Fans (b) numbered 61–68 blow air towards the ground.

Scheme 6: In Model 2, fans on the windward side blow air indoors (fans (a) numbered 1–15, 33–42); fans on the leeward side blow air outdoors (fans (a) numbered 17–32, 43–52). Fans (b) numbered 61–68 blow air towards the ground.

Scheme 7: In Model 2, fans (a) at a height of 9.6 m (odd-numbered fans on walls) blow air outdoors; fans at heights of 1 and 2 m (even-numbered fans on walls) blow air indoors. Fans (b) numbered 61–68 blow air towards the ground.

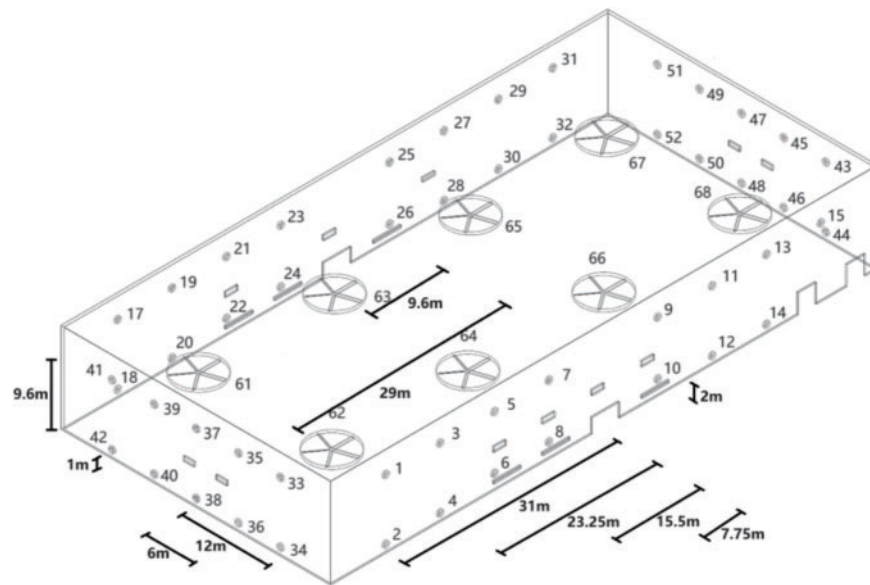
Scheme 8: In Model 2, fans (a) at a height of 9.6 m (odd-numbered fans on walls) blow air indoors; fans at heights of 1 and 2 m (even-numbered fans on walls) blow air outdoors. Fans (b) numbered 61–68 blow air towards the ground.

Fig. 7 illustrates the installation positions of the fans, which were strategically placed to maximize indoor airflow.



Model 1

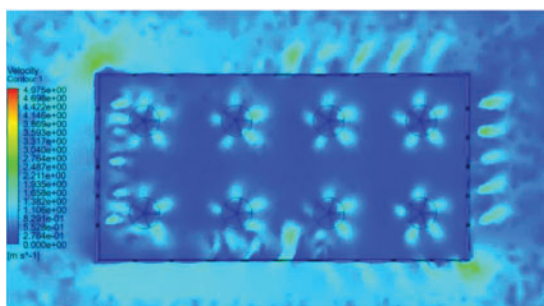
Figure 7: (Continued)



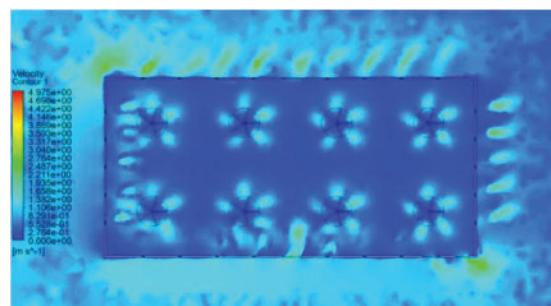
Model 2

Figure 7: Fan installation positions

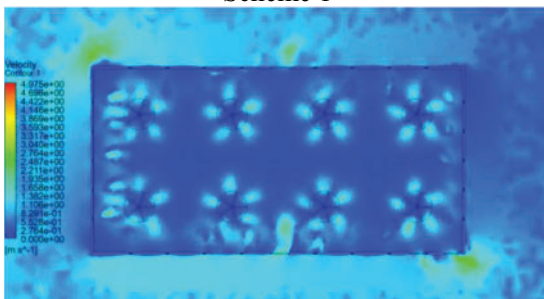
The wind speed contour maps for each design option, shown in Fig. 8, demonstrate the effects of different ventilation schemes at a height of 1.5 m:



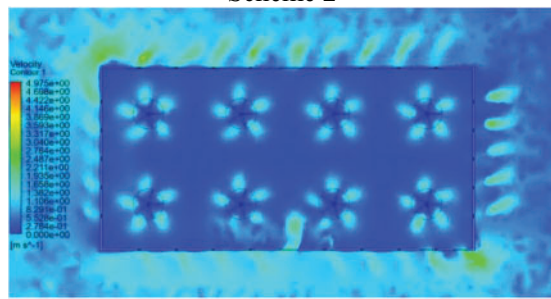
Scheme 1



Scheme 2



Scheme 3



Scheme 4

Figure 8: (Continued)

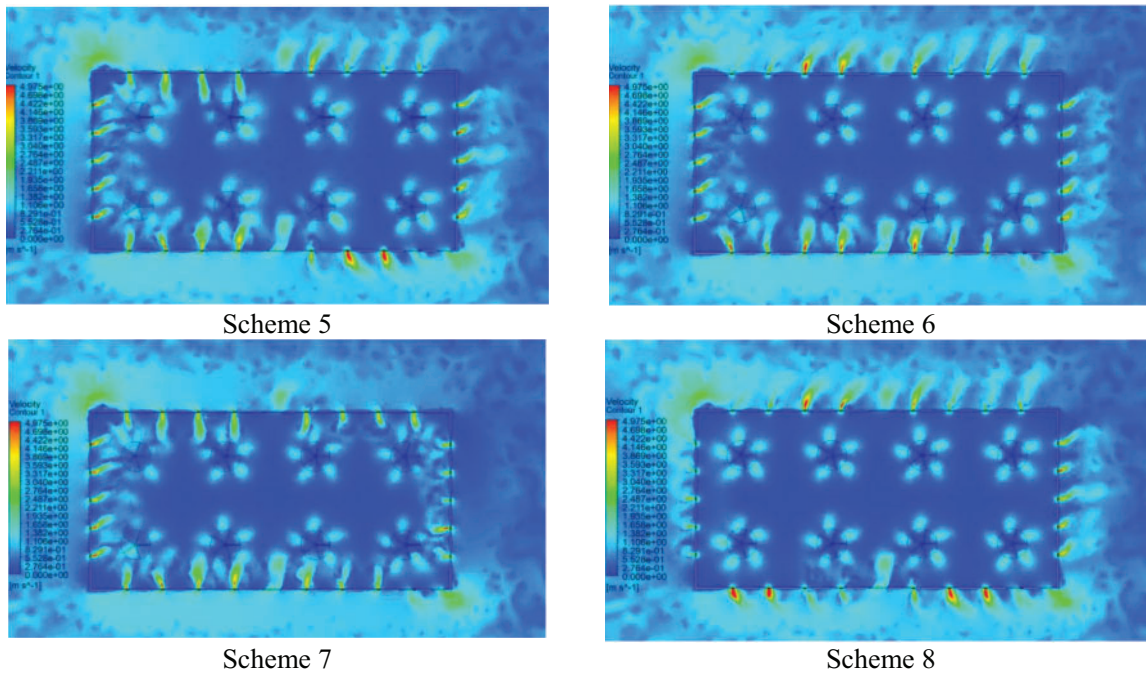


Figure 8: Wind speed contour maps by scheme

The simulation using Fluent for modelling airflow through the front and rear windows of the model shows the wind speed profiles. Please refer to Fig. 3 for the cross-sectional view of these profiles. Measurements of wind speed at a height of 1.5 m, with six sets of data for each scenario, analyzed as shown in Figs. 9 and 10.

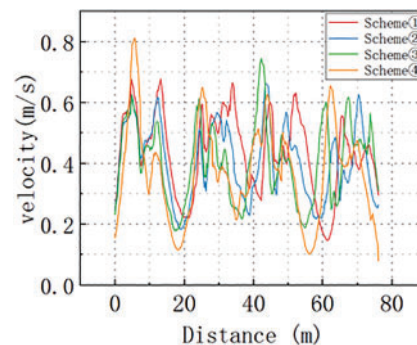


Figure 9: Comparison diagram of four schemes of Model 1

Fig. 9 shows that among the four schemes in Model 1, the average wind speed of Scheme 1 is 7.5% higher than Scheme 2, 7.6% higher than Scheme 3, and 16.4% higher than Scheme 4. Therefore, Scheme 1 is identified as the optimal scheme for Model 1. Fig. 10 shows that among the four schemes in Model 2, the average wind speed of Scheme 7 is 1.6% higher than Scheme 5, 11.5% higher than Scheme 6, and 34.3% higher than Scheme 8. Due to the very small difference between Scheme 5 and Scheme 7, both are determined to be the optimal schemes for Model 2.

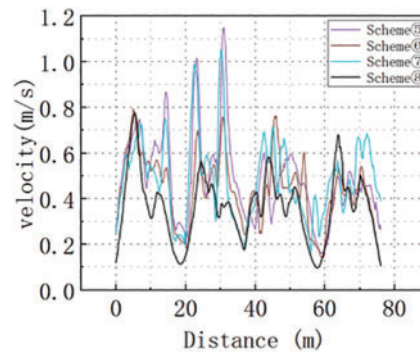


Figure 10: Comparison diagram of four schemes of Model 2

The analysis in Fig. 11 shows that the average wind speed for Scenario 7 is 1.6% higher than Scenario 5 and 12% higher than Scenario 1. Therefore, Option 7 was determined to be the best option. Since all fans are running at full speed, the fan speeds can be manually reduced to save energy while maintaining the required indoor air speeds for the gymnasium, which can be more easily observed through Fig. 12.

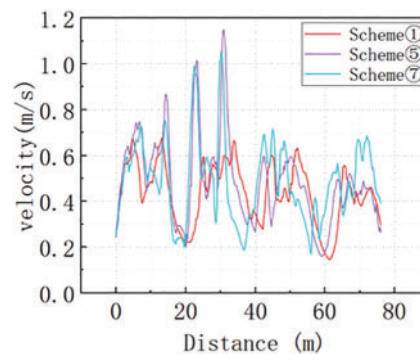


Figure 11: Comparison of the best scheme of the two models

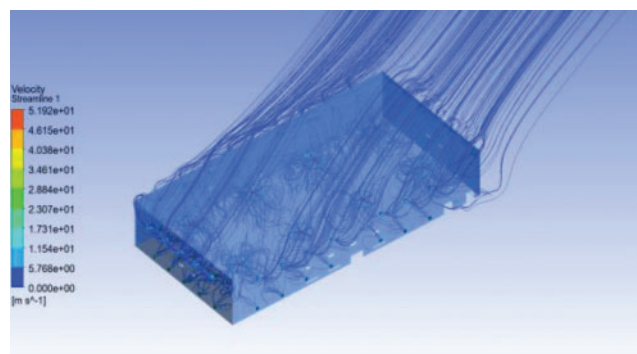


Figure 12: Streamline

Using numerical simulation, the average wind speed v (m/s) at the center points of windward doors and windows is selected to calculate the total area F (m²) of windward doors and windows.

Following the formula $L = 3600vF$, the hourly indoor air intake is calculated. Dividing this by the indoor volume V (m^3) of the sports hall, Scheme 7 achieves an air exchange rate of 3.73 times per hour [23], exceeding the requirement of 3 times per hour as per “Technical Specifications for Primary and Secondary School Sports Facilities” JGJ/T 280-2012. Using the same method, the air exchange rates per hour for each model were calculated, demonstrating that the optimal fan layout effectively increases indoor air exchange rates and improves indoor air quality.

Through analysis of Fig. 13, it is determined that after optimization, the average wind speed of Scheme 7 at a height of 1.5 m indoors is 276.7% higher than before. Comparison of indoor wind speeds before and after optimization:

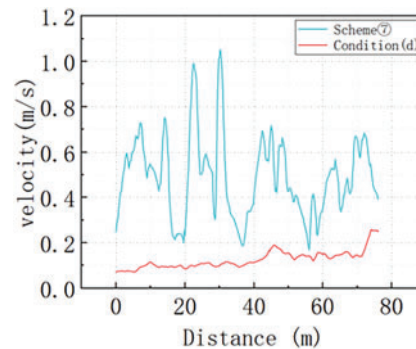


Figure 13: Wind speed analysis scheme at 1.5 m for each design option

As shown in Fig. 14, comparison of wind speed contour map before and after adding fan ($Z = 1.5$ m):

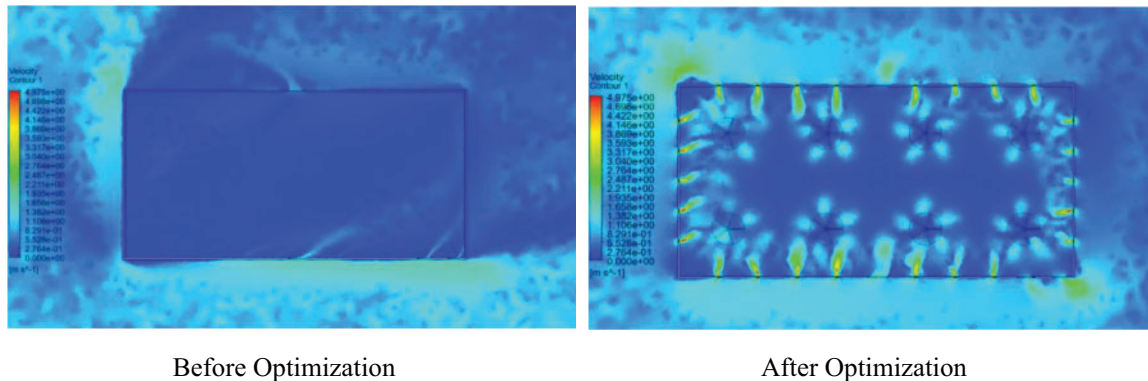


Figure 14: Comparison contour map of wind speeds at 1.5 m height

The average wind speed at a height of 1.5 m indoors in Scheme 7 reaches 0.489 m/s. Referring to Table 3, the optimization results in the average wind speed at a height of 1.5 m indoors changing from imperceptible to a level that makes occupants feel comfortable.

4 Discussion

Selection of Optimized Scenarios:

In Model 2, the average wind speed of Scenario 7 was found to be 1.6% higher than that of Scenario 5, 11.5% higher than that of Scenario 6, and 34.3% higher than that of Scenario 8, and thus Scenario 7 and Scenario 5 were determined to be the optimal scenarios for Model 2. Comparing the optimal solutions of the two models, it is found that the average wind speed of Solution 7 is 1.6% higher than that of Solution 5 and 12% higher than that of Solution 1, and therefore Solution 7 is determined to be the overall optimal solution.

Wind speed control:

Since all fans are running at full power, energy savings can be achieved by manually adjusting the fan speeds while maintaining the desired air flow rate in the gymnasium. Although the air velocity in some areas is relatively high, it can be controlled by adjusting the fan speed. Heat Stress Protection for Athletes. Athletes should be kept hydrated and cooled. Heat acclimatization is critical for athletes and should be part of the training program.

In this paper, by combining natural ventilation and mechanical exhaust, we design a scheme for optimal average indoor air velocity, which can reduce energy consumption, improve energy utilization, create a more comfortable environment for athletes and spectators, and promote health and well-being.

5 Conclusion

This study designed a numerical simulation of indoor air circulation in a university gymnasium with different exhaust ventilation methods and a new windward angle. By analyzing the indoor air velocity distribution under different working conditions, it was found that the air velocity distribution of working condition (d) is the most uniform, which can cover the indoor area more comprehensively, making it the optimal working condition. The analysis results further showed that the average air velocity of condition (d) is the highest, being 14.7% higher than that of condition (a), 8.59% higher than that of condition (b), and 18.7% higher than that of condition (c). Additionally, according to the national standard, the indoor wind speed should be controlled within the range of ≤ 1.0 m/s to meet the needs of human activities. Therefore, after installing fans, Scheme 7 (fans at 9.6 m height blowing outward on odd-numbered fans, and inward at 1 m and 2 m heights on even-numbered fans, with fans 61–68 blowing towards the ground) resulted in the highest indoor average wind speed. This optimization significantly increased the indoor air velocity, thus improving the indoor thermal environment and providing a more comfortable activity environment for athletes. Moreover, the average wind speed at a height of 1.5 m indoors increased by 276.7%, reaching a level perceived as comfortable. While wind speeds in some areas may be relatively high, they can be manually controlled by adjusting fan speeds.

In the future, the sustainable design concept of the stadium can be integrated into urban planning and construction, contributing to the construction of sustainable cities.

In this study, the optimization function of mechanical ventilation system is given full play to improve indoor thermal comfort and air quality. By rationally arranging fans, the average indoor wind speed can be significantly improved to make athletes feel comfortable, and it can also be used in the optimization of lees ventilation in the wine making industry. The influence of different building forms and ventilation system parameters on indoor thermal environment can be further explored in the future. Natural ventilation and mechanical ventilation will be combined to achieve a more environmentally friendly and energy-saving indoor environment control scheme, provide more comprehensive guidance for the design of sports venues, and promote the sustainable development of sports.

Only the thermal environmental conditions in summer were considered, but the conditions in other seasons were not involved, and the changes in indoor and outdoor temperatures were not studied. In the future, Ventilation optimization strategies in different seasons can be further explored to provide more comprehensive guidance for the year-round thermal environment regulation of sports venues. Future studies could be combined with physiological studies to more comprehensively assess the impact of ventilation optimization on athlete health and safety. This study only adopts the method of simulation analysis, which lacks the verification of actual field test. In the future, field experiments can be combined to verify the simulation results and improve the reliability of the research conclusions.

Acknowledgement: The authors acknowledge support from Fujian Key Laboratory of Intelligent Processing Technology and Equipment of Fujian University of Science and Technology and Provincial Department of Industry and Information Technology-Technological Innovation Key Research and Industrialization Project “High Performance Sintered Neodymium-Iron-Boron Permanent Magnet Manufacturing Equipment Research and Development and Application”.

Funding Statement: This research was supported by the Fujian Key Laboratory of Intelligent Processing Technology and Equipment at Fujian University of Technology and the Key Technical Innovation and Industrialization Project from the Provincial Department of Industry and Information Technology, titled “Research and Application of High-Performance Sintered Neodymium-Iron-Boron Permanent Magnet Manufacturing Equipment” (Project Number: 2023XQ002), under the leadership of Professor Xin Tong.

Author Contributions: Xuanzhong Wu: Review & editing, supervision, project administration, funding acquisition. Yanping Xiao: Writing—review & editing, writing—original draft, validation, investigation, formal analysis, data curation. All authors reviewed the results and approved the final version of the manuscript.

Availability of Data and Materials: Data will be made available on request.

Ethics Approval: This study did not involve any human or animal subjects, and therefore, ethics approval was not required.

Conflicts of Interest: The authors declare no conflicts of interest to report regarding the present study.

References

1. Esqueda H, Botello S, Valdez S. Estimation of peak flow in flood-producing rivers using numerical simulation, geospatial information and evolutionary algorithms. *Rev Int Métodos Numér Cálculo Diseño Ing.* 2024;40(3): 37, 1–24. doi:10.23967/j.rimni.2024.08.002.
2. Cao S, Zhao S, Ni Y, Jiao J. Design and structural analysis for a camber-morphing wing with deformable truss, *Métodos Numéricos Para Cálculo Y Diseño En Ingeniería. Revista Int.* 2024;40(2):1–10. doi:10.23967/j.rimni.2024.03.004.
3. Osorio M, Cordoba Florez L, Cruz A, Marulanda J, Thomson P. Comparison of wind loads on flat and gabled roofs calculated with the colombian building code and numerical results using CFD. *Rev Int Numer Methods Calc Eng Des.* 2019;35(2):29. doi:10.23967/j.rimni.2019.04.001.
4. Li J. Research on energy-saving design of daylighting and natural ventilation of university gymnasium based on system optimization. Harbin, China: Harbin Institute of Technology; 2010 (In Chinese).

5. Li J. Effect of form asymmetry of gymnasium on natural ventilation and thermal comfort of exercise site. *J South China Univ Technol.* 2013;41(3):83–89+107. doi:10.3969/j.issn.1000-565X.2013.03.012.
6. Zhao Y, Mei H. Study on optimization design of positions of ventilating windows for gymnasium buildings in the severe cold areas. *Build Sci.* 2014;30(2):83–8. doi:10.13614/j.cnki.11-1962/tu.2014.02.016.
7. Meng X, Wang Y, Xing X, Xu Y. Experimental study on the performance of hybrid buoyancy-driven natural ventilation with a mechanical exhaust system in an industrial building. *Energy Build.* 2020;208:109674. doi:10.1016/j.enbuild.2019.109674.
8. Elhadary M, Alzahrani A, Aly R, Elboshy B. A comparative study for forced ventilation systems in industrial buildings to improve the workers' thermal comfort. *Sustainability.* 2021;13(18):10267. doi:10.3390/su131810267.
9. Chen Y, Tong Z, Wu W, Samuelson H, Malkawi A, Norford L. Achieving natural ventilation potential in practice: control schemes and levels of automation. *Appl Energy.* 2019;235:1141–52. doi:10.1016/j.apenergy.2018.11.016.
10. Park B, Leen S. Investigation of the energy saving efficiency of a natural ventilation strategy in a multistory school building. *Energies.* 2020;13(7):1746. doi:10.3390/en13071746.
11. Bamdad K, Matour S, Izadyar N, Omrani S. Impact of climate change on energy saving potentials of natural ventilation and ceiling fans in mixed-mode buildings. *Build Environ.* 2022;209(10):108662. doi:10.1016/j.buildenv.2021.108662.
12. Heiselberg P. Principles of hybrid ventilation. In: Final report of IEA ECBCS Annex 35. Denmark: Aalborg Univ. (Denmark). Hybrid Ventilation Centre; 2002.
13. Gomis LL, Fiorentini M, Daly D. Potential and practical management of hybrid ventilation in buildings. *Energy Build.* 2021;231(2):110597. doi:10.1016/j.enbuild.2020.110597.
14. Pakari A, Ghani S. Comparison of different mechanical ventilation systems for dairy cow barns: CFD simulations and field measurements. *Comput Electron Agric.* 2021;186:106207. doi:10.1016/j.compag.2021.106207.
15. Li L, Wang C, Huang Y, Zhang L. Sensitivity analysis of building energy consumption of comprehensive gymnasium in cold region. *Build Energy Effic.* 2023;51, 386(04):1–11 (In Chinese).
16. Tang G. The traditional architecture of the Lingnan is adaptable to the hot-damp climate [Ph.D. dissertation]. Guangzhou, China: South China University of Technology; 2002 (In Chinese).
17. Wu Y, Chen Z, Yan X, Liu X. CFD numerical simulation on gymnasium roof of Liang du Sports Center. *Spatial Struct.* 2011;17(3):38–42 (In Chinese) doi:10.13849/j.issn.1006-6578.2011.03.008.
18. Chen Y, Wang X, Sun B, Li Q, Chen S. Wind tunnel experimental study on single room ventilation affected by miscellaneous factors. *J Zhejiang Univ (Eng Sci).* 2012;46(4):658–64. doi:10.3785/j.issn.1008-973X.2012.04.013.
19. Jiang Z, Kobayashi T, Yamanaka T, Sandberg M. A literature review of cross ventilation in buildings. *Energy Build.* 2023;291(1):113143. doi:10.1016/j.enbuild.2023.113143.
20. Park J. Long-term field measurement on effects of wind speed and directional fluctuation on wind-driven cross ventilation in a mock-up building. *Build Environ.* 2013;62:1–8. doi:10.1016/j.buildenv.2012.12.013.
21. Han Y, Liu Z, Feng B. Practice research on transformation of energy-efficient ventilation system in qiwu coal mine. *Coal Technol.* 2018;37(9):228–30 (In Chinese). doi:10.13301/j.cnki.ct.2018.09.085.
22. Nor Azli MNA, Hariri A, Chong ZY, Khasri MA, Muhamad Damanhuri AA, Syazwan Mustafa MS, et al. Influence of air velocity on thermal comfort and performance of students in naturally ventilated classrooms in tropical climate. *E3S Web Conf.* 2023;396:01116. doi:10.1051/e3sconf/202339601116.
23. Chen S, Cai Y, Jiang X. Unforced ventilation rate calculation under several conditions, Sichuan Build. *Sichuan Build Sci.* 2010;36(2):285–287+291.